

Voltage-Controlled Switching of Magnetic Anisotropy in Ambipolar Mn₂CoAl/Pd Bilayers

Yao Zhang^{1,2,3}, Guy Dubuis,^{2,4} Tane Butler,¹ Szymon Kaltenberg¹, Edward Trewick¹, and Simon Granville^{1,2,*}

¹ Robinson Research Institute, Victoria University of Wellington, Wellington, 6140 New Zealand

² MacDiarmid Institute for Advanced Materials and Nanotechnology, Wellington, 6012 New Zealand

³ School of Chemical and Physical Sciences, Victoria University of Wellington, Wellington, 6140 New Zealand

⁴ Now at Measurement Standards Laboratory, 69 Gracefield Road, Lower Hutt 5010, New Zealand



(Received 7 October 2021; revised 16 January 2022; accepted 15 February 2022; published 2 March 2022)

An ultrahigh electric field induced by ionic liquid gating (ILG) can be employed to manipulate ferromagnetism with low Joule heating dissipation, showing great potential for spintronics applications. In ferromagnetic/heavy metal thin films, however, typical materials used in both layers are electron-carrier dominant, which significantly suppresses the ILG effect due to the short electrostatic screening length in metal. Here, we employ Mn₂CoAl, a spin gapless semiconductor with hole carriers, as the ferromagnetic layer and investigate the ILG effect in MgO/Mn₂CoAl/Pd ultrathin films with perpendicular magnetic anisotropy. Reversible change of the magnetic anisotropy from the out-of-plane to the in-plane direction is achieved, induced by electrostatic charge accumulation. Moreover, ambipolar transport behavior has been observed and explained by a two-carrier model. Finally, we find that skew scattering is the mechanism of the anomalous Hall effect and can be enhanced at a positive gate voltage in our system. Our results strongly demonstrate that a significant ILG effect on magnetism can be easily achieved in two-carrier dominant ultrathin films.

DOI: 10.1103/PhysRevApplied.17.034006

I. INTRODUCTION

An exotic electronic band structure can induce various physical and chemical phenomena which are important not only for fundamental research but also for practical applications [1–3]. Recent studies have reported an interesting class of semiconductor materials exhibiting a partially gapless band structure at the Fermi level (E_F) [4, 5]. These materials, called spin gapless semiconductors (SGSs), exhibit a band gap in one of the spin channels and a zero-band gap in the other, as shown in Fig. 1(a) [6], which bridge the gap between semiconductors and half-metallic ferromagnets with a 100% spin polarization and show great potential for spintronics applications.

The SGS Mn₂CoAl was experimentally verified in 2013 [7]. This inverse Heusler compound shows a magnetic moment of $2\mu_B$ and a high Curie temperature of 720 K. In order to develop this material for spintronics applications, researchers are starting to extend the study of Mn₂CoAl from bulk to thin films [8–13]. Furthermore, perpendicular magnetic anisotropy (PMA) and skyrmions, a type of topological spin texture with nanoscale size, have been observed in MgO/Mn₂CoAl/Pd thin films due

to the strong spin-orbit coupling and Dzyaloshinskii-Moriya interaction (DMI) at the interface between the Pd and Mn₂CoAl layer [14–16], making this material more attractive to use in ultralow-power and ultrahigh-density devices [17,18].

Ionic liquid gating (ILG) using ionic liquids or ion gels has been demonstrated as a powerful method to effectively tune the ferromagnetism, superconductivity, and metal-insulator transition in thin films [19,20]. Using this method, an ultrahigh electric field can be generated at the electric double layer (EDL) interface over a nanometer-scale gap between the ions in the Helmholtz layer and charge carriers in the sample [20]. This interfacial gating behavior can lead to controlled and reversible changes of carrier concentration, and to a magneto-ionic effect [21]. For a ferromagnet/heavy metal system with PMA, the magnetic anisotropy, coercive field, and DMI can be tuned by ILG due to the electrostatic charging or magneto-ionic effect. Also, ILG can be used to control magnetic domains and generate skyrmions [22]. However, most of the work carried out has employed the Co and Co-Fe-B as the ferromagnetic layer and Ta, Pd, and Pt as the heavy metal layer [23–26]. These typical metallic materials used as both ferromagnetic and heavy metal layers exhibit a large electron-carrier concentration and short electrostatic

* simon.granville@vuw.ac.nz

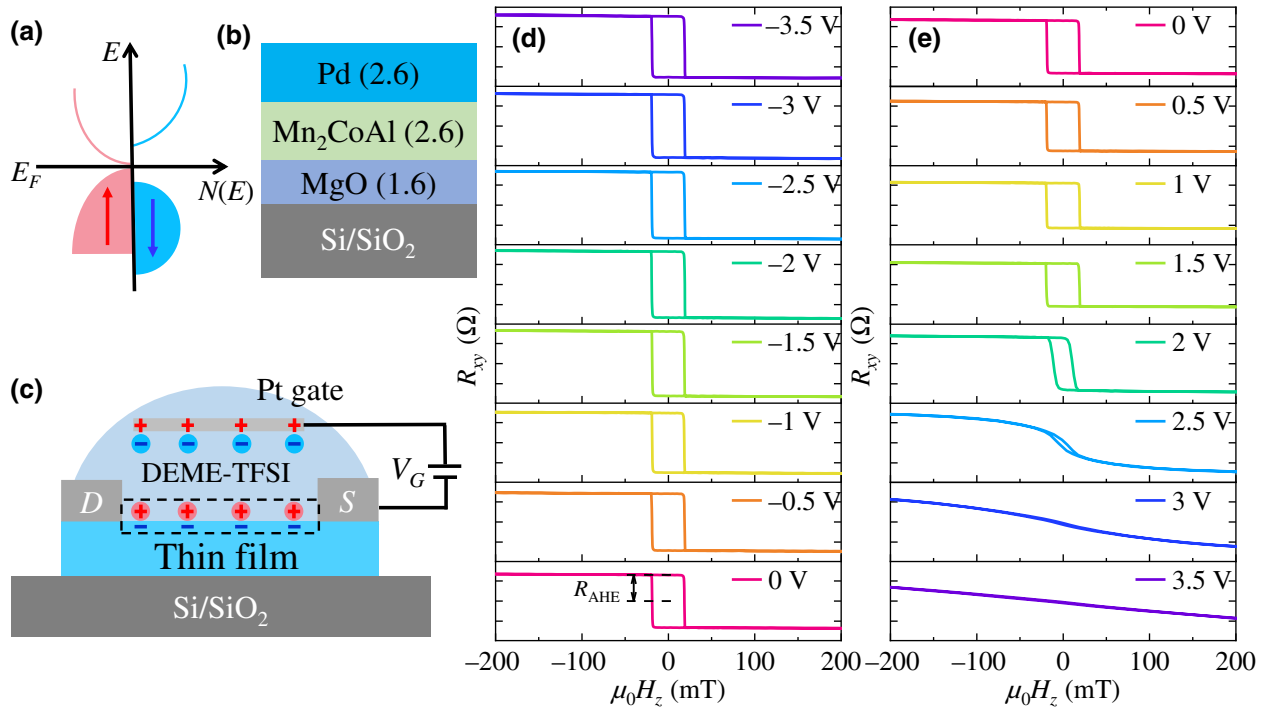


FIG. 1. (a) Schematic of density of states for an SGS. The density of states $N(E)$ as a function of energy E . The occupied states are indicated by filled areas. Arrows indicate the majority (\uparrow) and minority (\downarrow) states. (b),(c) Schematic of the thin-film structure and device, respectively. (d),(e) Typical gate dependence of AHE measured in an out-of-plane magnetic field at 150 K for a MgO(1.6 nm)/Mn₂CoAl(2.6 nm)/Pd(2.6 nm) stack.

screening length so that electrons cannot be entirely compensated in the top heavy metal by ILG, not to mention the modulation in the bottom ferromagnetic layer. Therefore, the ILG effect on the ferromagnetic layer can be dramatically suppressed.

On the other hand, in the two-carrier system combining materials with electronlike and holelike charge carriers, the anomalous Hall effect and magnetism can be observed [27–29]. It is known that the Mn₂CoAl thin film is a *p*-type material with a hole-carrier concentration (from approximately 1.6×10^{20} to $4 \times 10^{22} \text{ cm}^{-3}$ from different groups [13]), and ambipolar transport behavior induced by altering the polarization of dominant carriers has been observed by ILG [30]. Usually, heavy metals with electron carriers are needed to induce PMA, which has been shown in a Mn₂CoAl/Pd system [15]. Thus, the combination of holelike Mn₂CoAl and electronlike heavy metal Pd is unusual and may result in exotic magnetotransport phenomena not seen in structures made of conventional metals. Moreover, this two-carrier heterostructure is an ideal system for not only tuning the electronic states and E_F but also realizing ambipolar transport by ILG.

In this work we investigate the ILG effect in MgO/Mn₂CoAl/Pd ultrathin films with two carriers and PMA. We demonstrate that the magnetic anisotropy can be reversibly switched from the out-of-plane to the in-plane direction. The ambipolar transport behavior

also can be observed and elucidated by a two-carrier model.

II. EXPERIMENTAL METHOD

Ultrathin films consisting of MgO/Mn₂CoAl/Pd trilayers, as shown in Fig. 1(b), were deposited on thermally oxidized Si/SiO₂ (300 nm) substrates by magnetron sputtering with a base pressure below 4×10^{-8} torr. Samples were grown at ambient temperature while rotating the sample holder and then annealed *in situ* for 1 h at 300 °C. MgO was rf sputtered at a growth rate of 0.05 Å/s. Mn₂CoAl and Pd were dc sputtered at a growth rate of 0.84 Å/s and 0.46 Å/s, respectively. For more information of the sample fabrication, see our previous work [14,15]. A reference sample without a Mn₂CoAl layer, MgO(1.6 nm)/Pd(2.6 nm), has also been grown. Then trilayers were patterned into standard Hall bars ($l = 1600 \mu\text{m}$, $w = 150 \mu\text{m}$) by photolithography and then Ar ion milling. Ta(2 nm)/Cu(100 nm) were deposited as contact pads for electrical transport measurements. A small droplet of ionic liquid, N,N-Diethyl-N-methyl-N-(2-methoxyethyl)ammonium bis(trifluoromethylsulfonyl) imide (DEME-TFSI, IoLiTec), was used as the electrolyte connecting the Pt wire gate electrode and the Hall channel of the device, as shown in Fig. 1(c).

The gate voltage was applied and changed by a Keithley 6517B electrometer at $T = 220$ K, which is just above the glass transition temperature of DEME-TFSI. Because the interfacial chemistry is significantly suppressed at this transition temperature [31], any possible interfacial electrochemistry between the ionic liquid (IL) and Hall channel can be avoided. The charging route is $3.5\text{ V} \rightarrow -3.5\text{ V} \rightarrow 3.5\text{ V} \rightarrow 0\text{ V}$ with a step of 0.25 V or 0.5 V . All samples were charged for 30 min to reach the equilibrium of carriers at each gate voltage.

Anomalous Hall resistance and longitudinal resistance were measured at and below 175 K by using the resistivity option of a physical property measurement system (Quantum Design). It should be noted that the mobile ions in the IL were completely frozen and the gate current cannot be modulated by electrostatic gating voltage at temperatures below 175 K, therefore samples can be affected under the same ILG condition at a fixed gate voltage for temperature-dependent measurements.

III. RESULTS

A. Gate voltage-dependence of magnetic anisotropy

It is well known that the anomalous Hall effect (AHE) is a typical method for identifying the PMA and in-plane magnetic anisotropy (IMA) [17]. Usually, the Hall resistance is comprised of two terms, $R_{xy} = R_o H_z + R_A M_z$, where R_o and R_A are the ordinary and anomalous Hall coefficient, respectively. In ferromagnetic materials, R_A is much greater than R_o so that R_{xy} is usually proportional to the out-of-plane component of magnetization, M_z .

To investigate the magnetic anisotropy of trilayers influenced by ILG, the AHE of the $\text{MgO}(1.6\text{ nm})/\text{Mn}_2\text{CoAl}(2.6\text{ nm})/\text{Pd}(2.6\text{ nm})$ films was measured under various gate voltages (V_G) at 150 K, as shown in Figs. 1(d)–1(e). In the bottom panel of Fig. 1(d), there is a square hysteresis loop with a coercive field $\mu_0 H_c = 18.6$ mT and a saturation Hall resistance $R_s = 0.43\text{ }\Omega$ at $V_G = 0\text{ V}$, meaning that this trilayer exhibits a PMA. For an oxide–ferromagnet–heavy-metal system, the PMA usually originates from the electronic hybridization between the oxygen and magnetic transition metal orbit at the interface between the MgO and Mn_2CoAl , the spin-orbit interaction and the magnetic proximity effect at the interface of Mn_2CoAl and Pd [32]. By applying a negative V_G from 0 V to -3.5 V , the square shape of loops and $\mu_0 H_c$ of the sample is unchanged, as shown in Fig. 1(d). In the case of positive V_G [see Fig. 1(e)], the PMA of the sample is still robust under a relatively low V_G up to 1.5 V. However, the hysteresis loop starts to shrink at $V_G = 2\text{ V}$ and entirely disappears at $V_G = 3\text{ V}$. From our previous result that a clearly square hysteresis loop can be observed by sweeping the in-plane magnetic field if the out-of-plane hysteresis loop disappears induced by ILG [22], we believe that the

magnetic moments switch from the out-of-plane to the in-plane direction when V_G is greater than 2 V, rather than are reducing. After setting the voltage back to 0 V, the PMA is spontaneously recovered with a loop in which $\mu_0 H_c$ is indistinguishable from the first 0 V loop, meaning that the ILG effect in our system is reversible (see Fig. S1 in the Supplemental Material [33]).

The density of states of nonmagnetic Pd or Pt at the Fermi energy nearly satisfies the Stoner criterion in which the ferromagnetism is expected to occur when $N(E_F)I > 1$, where N and I are the density of states at the Fermi energy and Stoner parameter, respectively [34,35]. Recently, it has been experimentally demonstrated that magnetization can be induced in Pt and Pd thin films by ILG [36–38]. To check if any component of the AHE we measure in the trilayers is from the Pd layer magnetized by ILG, a reference sample without a Mn_2CoAl layer, $\text{MgO}(1.6\text{ nm})/\text{Pd}(2.6\text{ nm})$, has been studied under different gate voltages. However, we find no evidence of AHE observed from 175 K to 3 K at either positive or negative voltages (see Fig. S2 in the Supplemental Material [33]). Therefore, we can rule out the presence of a magnetization in the Pd induced by the ILG, and the AHE effects we detect are from the ferromagnetic Mn_2CoAl layer.

B. Ambipolar transport behavior

To comprehensively understand the ILG influence on the magnetic behavior of the Mn_2CoAl trilayer, the crucial parameters were extracted from the anomalous Hall hysteresis loops or longitudinal resistance (R_{xx}) curves, as shown in Fig. 2. Figure 2(a) shows the ratio of remanent Hall resistance and saturation Hall resistance, R_r/R_s . Starting with V_G at 3.5 V, the value of the ratio is 0, that is, the magnetic moments are along the in-plane direction. When changing V_G toward -3.5 V , R_r/R_s becomes 1 when V_G reaches the voltage threshold for the onset of PMA, about 1.75 V. Then, by setting V_G back toward 3.5 V, the PMA disappears again at a threshold voltage of 1 V. Figure 2(b) displays the gate dependence of $\mu_0 H_c$ measured from the anomalous Hall loops, showing a similar behavior to R_r/R_s . $\mu_0 H_c$ is 19 mT for the sample in the PMA state, with a significant reduction of 84% to 3 T when the sample changes to IMA.

The gate dependence of saturation anomalous Hall resistance (R_{AHE}) is presented in Fig. 2(c) after subtracting the ordinary Hall effect with an R_o from -1.05 to $-1.26 \times 10^4\text{ cm}^3\text{ C}^{-1}$ at various V_G . It firstly shows an M-shape with a minimum value of $0.36\text{ }\Omega$ at 1.25 V when changing V_G from 3.5 to -3.5 V [see the black curve in Fig. 2(c)], and then when changing V_G back to 3.5 V, R_{AHE} increases to a maximum value of 0.72Ω at 2 V before flattening off at higher V_G . We also repeated the voltage change from 3.5 to 0 V; the plot of R_{AHE} versus V_G [see the blue curve in Fig. 2(c)] shows a similar trend to that of the first gate

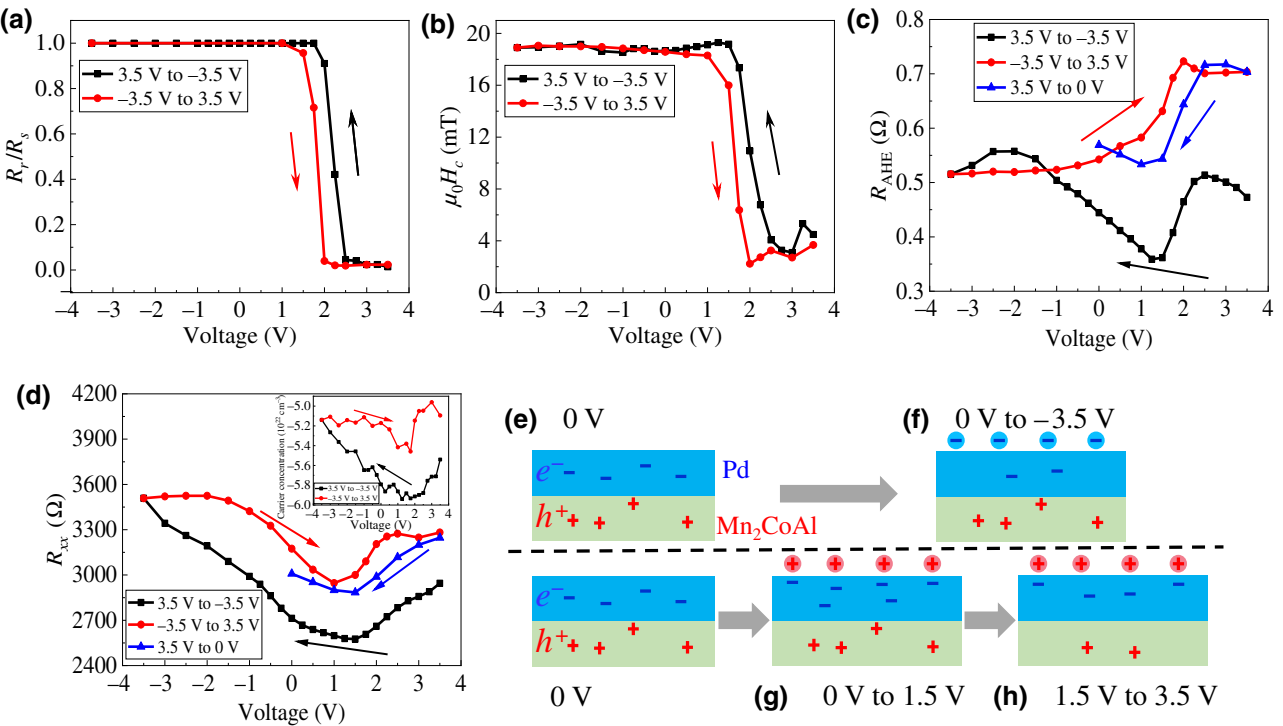


FIG. 2. (a)–(d) Gate dependence of R_r/R_s , $\mu_0 H_c$, R_{AHE} and R_{xx} , respectively, at 150 K. The inset of (d) shows the carrier concentration as a function of gate voltage. (e)–(h) The state of two-carrier model for 0 V, 0 V to -3.5 V, 0 V to 1.5 V, and 1.5 V to 3.5 V, respectively. The e^- (–) and h^+ (+) correspond the electron and hole carrier. Anions (\ominus) and cations (\oplus) are accumulated on the surface of Pd in (f),(g), respectively.

voltage sweep (black curve), only with an upward shift compared to the first sweep. Like other inverse Heusler alloys with itinerant electron magnetism [39], the intrinsic magnetic properties of Mn₂CoAl are primarily determined by unpaired d electrons of Mn and Co elements with energies close to E_F [5]. It is known that the value of magnetization or R_{AHE} can be tuned by shifting the position of E_F . [10,40]. Since the R_{AHE} was extracted under an out-of-plane saturation magnetic field the magnetization is always in the out-of-plane direction and there is no influence on R_{AHE} from spin reorientation. Therefore, we think the change in R_{AHE} might be ascribed to the modification of electron density at E_F by the ILG-induced electrical field.

For metals with electron carriers, like Pt and Au, R_{xx} shows a linear relationship with V_G [41,42]. In our system, the gate dependence of R_{xx} measured at zero magnetic field exhibits this linear association from -3.5 to 1.5 V, as shown in the black curve of Fig. 2(d). However, R_{xx} starts to increase for V_G above 1.5 V, meaning that some of the carriers have been compensated and start to change polarity, which can be called ambipolar transport behavior [20]. The change in R_{xx} is in line with the behavior of the gate dependence of carrier concentration; see the black curve of inset of Fig. 2(d). After setting V_G back to 3.5 V [see the red curve of Fig. 2(d)], the ambipolar characteristics of R_{xx} can still be observed with an upward shift compared

with the black curve of Fig. 2(d). One can also see that R_{xx} is almost unchanged in the range from -3.5 to -1.5 V. This hysteresis results from the slow restructuring process of ions or polarization relaxation of the EDL, that is, the carriers are almost locked [43,44], which can be confirmed in the red curve of the inset of Fig. 2(d) where the carrier concentration is nearly unchanged in the same regime. This locked-carrier effect induces the upward shift of R_{xx} . It is quite notable that the minimum values of R_{xx} in the red and black curves of Fig. 2(d) are reached at a V_G of 1 V and 1.5 V, respectively, almost identical to the voltage thresholds for the change between PMA and IMA states in Figs. 2(a) and 2(b).

Though there is a difference of R_{xx} between magnetization parallel and perpendicular to the electrical current, which is the so-called anisotropic magnetoresistance effect, this effect is very small for $3d$ ferromagnetic materials, usually less than 5% [45], and in Mn₂CoAl films it is less than 0.4% [46]. For our case, there is an 8.6% difference in R_{xx} between 0 and 3.5 V, where the spin-reorientation transition happens. Furthermore, R_{xx} enhances 29.3% at -3.5 V, where the magnetization is still in the perpendicular direction. This significant change cannot be ascribed to the spin-reorientation transition. Therefore, we conclude the change in R_{xx} is mostly affected by the carrier concentration.

It should be noted that these results as shown in Figs. 2(c) and 2(d) in our heterostructures are different from other PMA systems in which the charge carriers of both ferromagnetic and heavy metal layers are electrons. In our system, the Mn₂CoAl layer is hole-carrier dominant (see Fig. S3 in the Supplemental Material [33]) while the top Pd layer is electron-carrier dominant (see Fig. S2 in the Supplemental Material [33]). Therefore, we establish a simple two-carrier model to explain this ambipolar transport behavior and magnetic properties as a function of V_G , as shown in Figs. 2(e)–2(h). At 0 V, there are free electrons and holes in the Pd and Mn₂CoAl layer, respectively, as shown in Fig. 2(e). With increasing V_G in the negative gate direction, anions are accumulated above the film surface and thus decrease the number of electron carriers in the Pd layer, resulting in an increase in R_{xx} with less electron conduction, as shown in Fig. 2(f). Since the Pd thin film shows a very high electron-carrier concentration, $8.7 \times 10^{22} \text{ cm}^{-3}$ [see Fig. S2(c) in the Supplemental Material [33]] and all electrons in the Pd layer cannot be depleted at this intermediate V_G , we believe that the carriers in the Mn₂CoAl layer are not affected. On the other hand, when the Hall channel is positively biased, the electron concentration increases in the Pd associated with the decrease in R_{xx} , as shown in Fig. 2(g). This gate-dependent behavior of R_{xx} is in line with other metals that also have electrons as the charge carriers [41,42]. However, when subsequently increasing the V_G above 1.5 V, some of the electrons might diffuse into the Mn₂CoAl layer so that some of the positive carriers in that layer are compensated. Therefore, R_{xx} starts to increase and exhibits an ambipolar transport behavior. This behavior has also been observed in thick Mn₂CoAl films by ILG [30]. As we mentioned above, the voltage threshold for the change between PMA and IMA relates to the minimum value of R_{xx} . We think the hole carriers start to be depleted in the Mn₂CoAl layer at these minimum V_G points and change the interface interaction.

It must be stressed that the chemical window of DEME-TFSI is as high as 6 V when charging at the glass transition temperature, 220 K [47]. Though in Fig. 2(d) the value of R_{xx} does not return to the initial state at 3.5 V after cycling of the V_G , we think the reason is the slow polarization relaxation of the EDL [43,44] rather than the electrochemical reaction. Moreover, the characteristic of gate dependent R_{xx} is reversible. All the foregoing strongly suggests that there is no irreversible electrochemical reaction at 3.5 V in our system.

C. Temperature dependence of magnetotransport

We also investigated the ILG effect on the magnetotransport behavior at different temperatures from 175 K to 3 K at V_G values of -3.5 V , -0.75 V and 3.5 V , respectively, as shown in Fig. 3. The sample shows a robust PMA from 175 K to 3 K with a V_G at -3.5 V and -0.75 V , respectively, as shown in Figs. 3(a) and 3(b). In the case of $V_G = 3.5 \text{ V}$, hysteresis appears with a creeping transition near the coercive field when decreasing the temperature because the effective perpendicular magnetic anisotropy of ultrathin films increases greatly with decreasing temperature [48], as shown in Fig. 3(c).

The values of $\mu_0 H_c$ and R_{AHE} were extracted from Fig. 3, as shown in Figs. 4(a) and 4(b), respectively. Both rise with decreasing temperature. Comparing the value of $\mu_0 H_c$ at -3.5 V and -0.75 V , it is the same from 175 K to 100 K. However, $\mu_0 H_c$ is greater at -3.5 V from 75 to 3 K, implying that the ILG effect is enhanced at low temperature. Regarding $\mu_0 H_c$ at 3.5 V , it is smaller than at -3.5 V and -0.75 V at all temperatures due to the reduction of PMA induced by the ILG effect. Turning to the temperature dependence of R_{AHE} , R_{AHE} rises by cooling the sample for all V_G , but the values for a positive V_G are significantly higher, around 42%–45% greater than the values for $V_G = -0.75 \text{ V}$ from 175 K to 3 K. Though thick Mn₂CoAl layers show a weakly semiconducting behavior

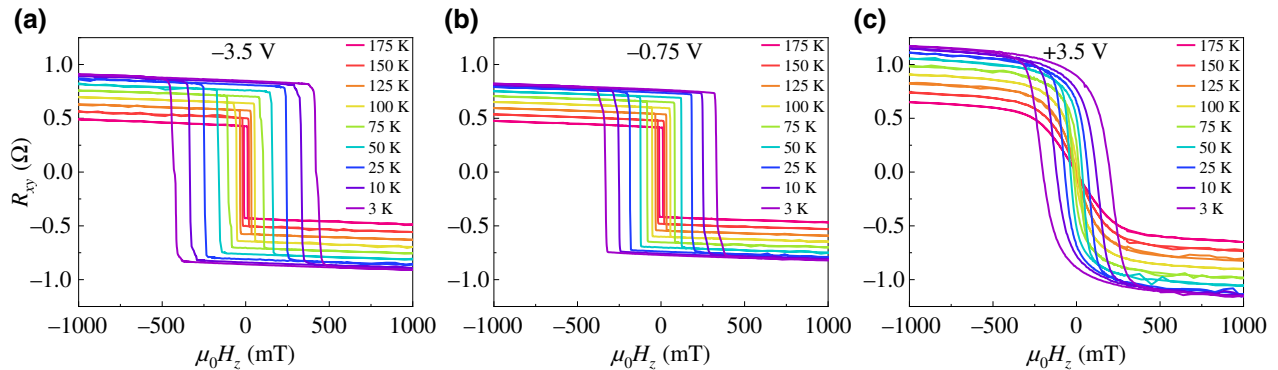


FIG. 3. The AHE of the MgO(1.6 nm)/Mn₂CoAl(2.6 nm)/Pd(2.6 nm) stack measured from 175 K to 3 K at -3.5 , -0.75 , and 3.5 V , respectively.

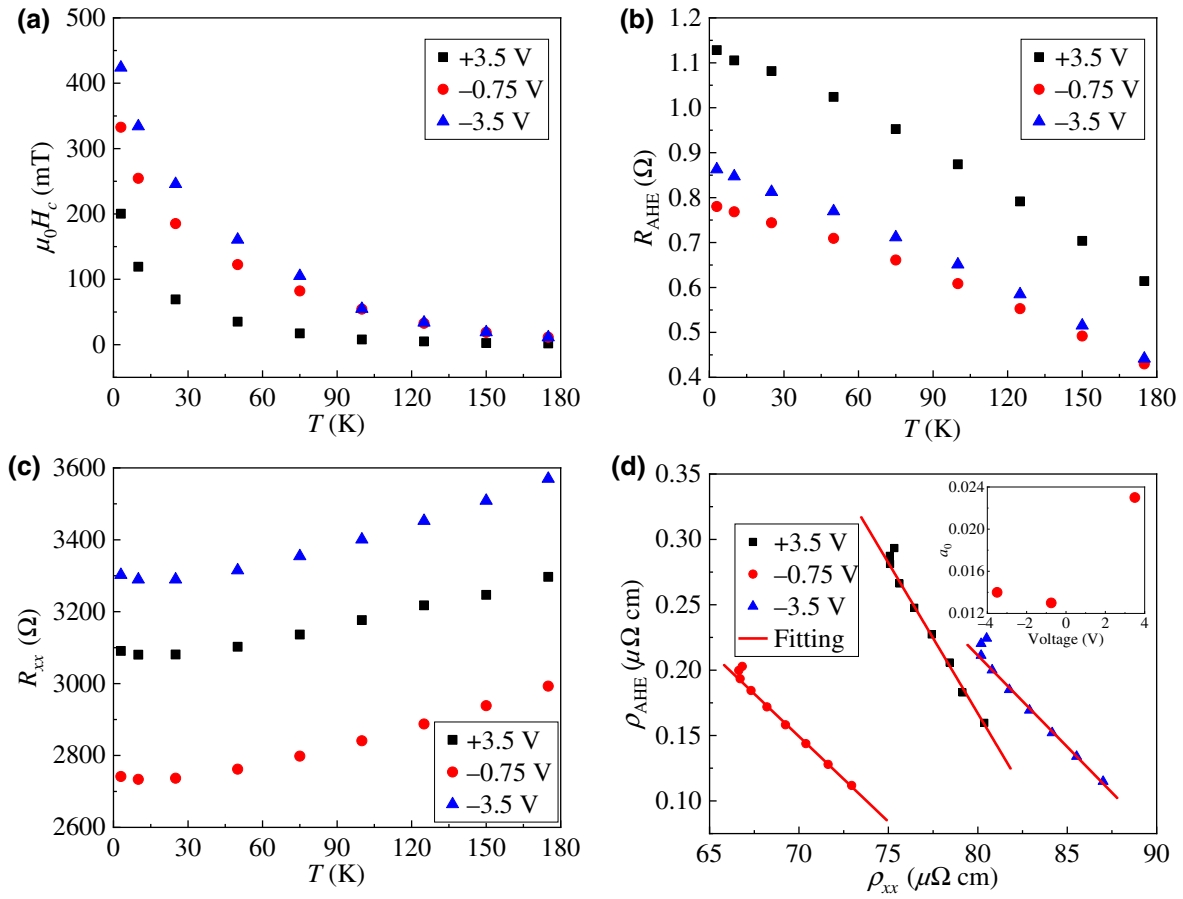


FIG. 4. (a)–(c) Temperature dependence of $\mu_0 H_c$, R_{AHE} , and R_{xx} , respectively, from 175 K to 3 K at -3.5 , -0.75 , and 3.5 V. (d) Gate dependent plot of ρ_{AHE} versus ρ_{xx} . The inset shows the skew-scattering parameter a_0 as a function of gate voltage.

[see Fig. S3(b) in the Supplemental Material [33]], the temperature dependence of R_{xx} in the stacks exhibits a typical metallic behavior with a residual resistance around 15 K, as shown in Fig. 4(c), suggesting that the carrier concentration and conductivity of Pd are greater than that of Mn_2CoAl in the ultrathin film stacks.

By plotting ρ_{AHE} versus ρ_{xx} , one can identify the mechanisms of AHE in ultrathin multilayer systems [49–51]. Figure 4(d) is the $\rho_{\text{AHE}}-\rho_{xx}$ plot for the sample measured at 175 K to 3 K at -3.5 V, -0.75 V, and 3.5 V, respectively. Interestingly, a nicely linear dependence on ρ_{xx} can be observed in the range from 175 K to 25 K. We notice that this unusually linear behavior has been reported in some other materials. For instance, in thin films of Ni, granular Ni-SiO₂ mixtures, and Co nanoclusters embedded in Pt matrix [52], skew scattering, an asymmetric scattering of electrons by impurities, is considered as the mechanism giving rise to the linear dependence due to the surface scattering or nonmagnetic impurities. Considering that there is an unavoidable mixture of Pd and Mn_2CoAl at the interface, the nonmagnetic Pd impurity might be one of the sources of skew scattering because Pd showing a strong spin-orbit interaction is able to induce the

difference in the skew-scattering probabilities for spin-up and spin-down electrons. Furthermore, a theory about the chiral spin fluctuation induced by the impurity has been reported to clarify the linear relationship in ILG SrCoO₃ thin films [53]. Recently, Ishizuka *et al.* reported that skew scattering can also be induced by spin chirality in a system with DMI [54]. In our previous work [15,22], a DMI of 0.2 – 0.35 mJ m⁻² has been proved at the interface between the Pd and Mn_2CoAl layer due to the broken inversion symmetry and strong spin-orbit coupling. Therefore, we expect spin chirality to be another source of skew scattering in our system.

When skew scattering dominates, both ρ_{AHE} and ρ_{xx} are proportional to the transport lifetime and thus $\rho_{\text{AHE}} = a_0 \rho_{xx}$ [55], where a_0 is the skew-scattering parameter, meaning the strength of the scattering. By fitting these results with this linear equation, one can obtain a skew-scattering parameter a_0 of 0.014 , 0.013 , and 0.023 for -3.5 V, -0.75 V, and 3.5 V, respectively, as shown in the inset of Fig. 4(d). This nice linear fit leads to a very low uncertainty, approximately 10^{-5} . The skew-scattering effect is almost unchanged at $V_G = -3.5$ V. From the model we established in Fig. 2, the number of carriers is

only changed in the Pd layer and there is no influence in the Mn₂CoAl layer. As a result there is no effect of V_G on the spin-dependent skew scattering in the ferromagnetic layer. However, there is a strong enhancement, 76.9%, of skew scattering at positive $V_G = 3.5$ V. This may be related to the two-carrier model in which the electrons diffuse into Mn₂CoAl and thus increase the possibility of skew scattering. The advantage of this two-carrier heterostructure is that the strength of skew scattering can be easily changed by only tuning the carrier concentration without doing any chemical doping which can change the level of disorder.

IV. DISCUSSION

Here, we discuss the origin of the magnetic anisotropy switch due to the gating voltage as shown in Figs. 1 and 2. Conventionally, there are three potential effects of ILG: electrostatic charging, magneto-ionic effects, and electrochemical reactions [21]. But only electrostatic charging effects exhibits a volatile and reversible behavior after switching off the gate voltage. Electrostatic charging is due to carriers accumulating at the surface which generate a volatile ultrahigh electric field in the trilayer. With this electric field, Zhao *et al.* found that the distribution of the charge density in a heavy metal can be varied, resulting in a changing of the spin-orbit coupling energy and a Rashba effect in a Au/DEME-TFSI/Pt/(Co/Pt)₂/Ta capacitor heterostructure with PMA [25]. For the Rashba effect, the spin degeneracy is removed under an electric field due to the spin-orbit interaction and leads to an effective in-plane magnetic field [56]. Considering that our films have a similar ferromagnetic/heavy metal structure to the PMA films of Ref. [25] and our previous work found that reversible and electrostatic changes in anisotropy can be observed under a small positive voltage [22], the origin can be potentially ascribed to the in-plane net Rashba field that causes the easy axis to change from the out-of-plane to the in-plane direction in a reversible mode.

To date, there has been lots of work on the modification of PMA in ferromagnetic-metal-heavy-metal systems by electrostatic ILG. However, the electrostatic charging effect on the modification of PMA in these ferromagnetic metal systems is not as strong as in our trilayers that incorporate a Mn₂CoAl SGS. For instance, in ferromagnetic metals with PMA, the gate voltage does not completely switch the magnetic anisotropy to the in-plane direction and an out-of-plane hysteresis still exists [25,57–59]. To have a large modification of PMA by ILG, the number of carriers in the ferromagnetic layer needs to be modulated. Though the electron carrier concentration may increase in the ferromagnetic layer resulting from the electron diffusion from the heavy metal layer at positive gate voltages, the ferromagnet electron concentration cannot be significantly reduced since the heavy metal on the top already has a high concentration of electrons. To prove this

hypothesis, we prepared a PMA stack where we replaced the Mn₂CoAl layer with a layer of Co₂MnGa. The latter is a ferromagnet with an electron carrier concentration approximately $2 \times 10^{22} \text{ cm}^{-3}$, typical for metals [60,61], MgO(1.6 nm)/Co₂MnGa(3.0 nm)/Pd(2.5 nm). In Fig. S4 in the Supplemental Material [33], one can observe that the coercive field is almost unchanged at 3.5 V and can only be slightly tuned by ILG at a large positive $V_G = 5$ V. Though the coercive field of a Co₂MnGa stack is almost 10 times greater than that of a Mn₂CoAl stack at 175 K, the coercive field of the Mn₂CoAl stack shows a similar value at 25 K, as shown in Figs. 3(a) and 3(b), where the coercive field can be significantly tuned at 3.5 V. These results support the conclusion that the large ILG effect on the magnetic anisotropy we have observed is due to the bipolar conduction in the Mn₂CoAl/Pd heterostructure.

V. CONCLUSION

In summary, we employ the SGS Mn₂CoAl with dominant hole carriers as the ferromagnetic layer to fabricate two-carrier MgO/Mn₂CoAl/Pd ultrathin films with PMA and investigate their magnetic properties affected by ILG. The magnetic anisotropy of trilayers can be tuned from the out-of-plane to the in-plane direction under a positive gate voltage because an electrostatic charge accumulation happens at the surface and could induce a sufficient in-plane net Rashba magnetic field. We also observe an ambipolar transport behavior related to the onset of PMA which can be explained by a two-carrier model. Finally, the temperature-dependent magnetotransport of trilayers has been investigated. The Pd impurity and spin chirality might be the sources for the skew scattering leading to the AHE. The gate-dependent strength of skew scattering can also be elucidated by the two-carrier model. Our results strongly demonstrate that the two-carrier ultrathin film is an ideal system for the modification of ferromagnetism by the ILG.

ACKNOWLEDGMENTS

The MacDiarmid Institute is supported under the New Zealand Centres of Research Excellence Programme.

-
- [1] T. Ohta, A. Bostwick, T. Seyller, K. Horn, and E. Rotenberg, Controlling the electronic structure of bilayer graphene, *Science* **313**, 951 (2006).
 - [2] M. Katsnelson, V. Y. Irkhin, L. Chioncel, A. Lichtenstein, and R. A. de Groot, Half-metallic ferromagnets: From band structure to many-body effects, *Rev. Mod. Phys.* **80**, 315 (2008).
 - [3] N. Armitage, E. Mele, and A. Vishwanath, Weyl and dirac semimetals in three-dimensional solids, *Rev. Mod. Phys.* **90**, 015001 (2018).

- [4] X. Wang, Proposal for a new Class of Materials: Spin Gapless Semiconductors, *Phys. Rev. Lett.* **100**, 156404 (2008).
- [5] S. Skaftouros, K. Özdogan, E. Şaşioğlu, and I. Galanakis, Search for spin gapless semiconductors: The case of inverse heusler compounds, *Appl. Phys. Lett.* **102**, 022402 (2013).
- [6] X. Wang, Z. Cheng, G. Zhang, H. Yuan, H. Chen, and X.-L. Wang, Spin-gapless semiconductors for future spintronics and electronics, *Phys. Rep.* **888**, 1 (2020).
- [7] S. Ouardi, G. H. Fecher, C. Felser, and J. Kübler, Realization of Spin Gapless Semiconductors: The Heusler Compound Mn₂CoAl, *Phys. Rev. Lett.* **110**, 100401 (2013).
- [8] M. E. Jamer, B. A. Assaf, T. Devakul, and D. Heiman, Magnetic and transport properties of Mn₂CoAl oriented films, *Appl. Phys. Lett.* **103**, 142403 (2013).
- [9] G. Xu, Y. Du, X. Zhang, H. Zhang, E. Liu, W. Wang, and G. Wu, Magneto-transport properties of oriented Mn₂CoAl films sputtered on thermally oxidized si substrates, *Appl. Phys. Lett.* **104**, 242408 (2014).
- [10] K. Arima, F. Kuroda, S. Yamada, T. Fukushima, T. Oguchi, and K. Hamaya, Anomalous Hall conductivity and electronic structures of si-substituted Mn₂CoAl epitaxial films, *Phys. Rev. B* **97**, 054427 (2018).
- [11] R. G. Buckley, T. Butler, C. Pot, N. M. Strickland, and S. Granville, Exploring disorder in the spin gapless semiconductor Mn₂CoAl, *Mater. Res. Express* **6**, 106113 (2019).
- [12] Z. Chen, W. Liu, P. Chen, X. Ruan, J. Sun, R. Liu, C. Gao, J. Du, B. Liu, and H. Meng, *et al.*, Direct observation of ferrimagnetic ordering in inverse heusler alloy Mn₂CoAl, *Appl. Phys. Lett.* **117**, 012401 (2020).
- [13] K. Kudo, A. Masago, S. Yamada, L. Kumara, H. Tajiri, Y. Sakuraba, K. Hono, and K. Hamaya, Positive linear magnetoresistance effect in disordered L₂₁ B-type Mn₂CoAl epitaxial films, *Phys. Rev. B* **103**, 104427 (2021).
- [14] B. Ludbrook, G. Dubuis, A.-H. Puichaud, B. Ruck, and S. Granville, Nucleation and annihilation of skyrmions in Mn₂CoAl observed through the topological Hall effect, *Sci. Rep.* **7**, 13602 (2017).
- [15] Y. Zhang, G. Dubuis, T. Butler, and S. Granville, Fractal Analysis of Skyrmions Generated by Field-Assisted Fine-Tuning of Magnetic Anisotropy, *Phys. Rev. Appl.* **15**, 014020 (2021).
- [16] N. Sun, Y. Zhang, H. Fu, W. Che, C. You, and R. Shan, Perpendicular magnetic anisotropy in Mn₂CoAl thin film, *AIP Adv.* **6**, 015006 (2016).
- [17] B. Dieny and M. Chshiev, Perpendicular magnetic anisotropy at transition metal/oxide interfaces and applications, *Rev. Mod. Phys.* **89**, 025008 (2017).
- [18] X. Zhang, Y. Zhou, K. M. Song, T.-E. Park, J. Xia, M. Ezawa, X. Liu, W. Zhao, G. Zhao, S. Woo, Skyrmion-electronics: Writing, deleting, reading and processing magnetic skyrmions toward spintronic applications, *J. Phys.: Condens. Matter* **32**, 143001 (2020).
- [19] A. Goldman, Electrostatic gating of ultrathin films, *Annu. Rev. Mater. Res.* **44**, 45 (2014).
- [20] S. Z. Bisri, S. Shimizu, M. Nakano, and Y. Iwasa, Endeavor of iontronics: From fundamentals to applications of ion-controlled electronics, *Adv. Mater.* **29**, 1607054 (2017).
- [21] C. Navarro-Senent, A. Quintana, E. Menéndez, E. Pellicer, and J. Sort, Electrolyte-gated magnetoelectric actuation: Phenomenology, materials, mechanisms, and prospective applications, *APL Mater.* **7**, 030701 (2019).
- [22] Y. Zhang, G. Dubuis, C. Doyle, T. Butler, and S. Granville, Nonvolatile and Volatile Skyrmion Generation Engineered by Ionic Liquid Gating in Ultrathin Films, *Phys. Rev. Appl.* **16**, 014030 (2021).
- [23] Y. Liu, S. Ono, G. Agnus, J.-P. Adam, S. Jaiswal, J. Langer, B. Ocker, D. Ravelosona, and L. Herrera Diez, Electric field controlled domain wall dynamics and magnetic easy axis switching in liquid gated CoFeB/MgO films, *J. Appl. Phys.* **122**, 133907 (2017).
- [24] S. Zhao, Z. Zhou, B. Peng, M. Zhu, M. Feng, Q. Yang, Y. Yan, W. Ren, Z.-G. Ye, and Y. Liu, *et al.*, Quantitative determination on ionic-liquid-gating control of interfacial magnetism, *Adv. Mater.* **29**, 1606478 (2017).
- [25] S. Zhao, L. Wang, Z. Zhou, C. Li, G. Dong, L. Zhang, B. Peng, T. Min, Z. Hu, and J. Ma, *et al.*, Ionic liquid gating control of spin reorientation transition and switching of perpendicular magnetic anisotropy, *Adv. Mater.* **30**, 1801639 (2018).
- [26] L. H. Diez, Y. Liu, D. A. Gilbert, M. Belmeguenai, J. Vogel, S. Pizzini, E. Martinez, A. Lamperti, J. Mohammedi, and A. Laborieux, *et al.*, Nonvolatile Ionic Modification of the Dzyaloshinskii-Moriya Interaction, *Phys. Rev. Appl.* **12**, 034005 (2019).
- [27] J. Berry, S. Potashnik, S. Chun, K. Ku, P. Schiffer, and N. Samarth, Two-carrier transport in epitaxially grown MnAs, *Phys. Rev. B* **64**, 052408 (2001).
- [28] V. Tran, S. Paschen, R. Troć, M. Baenitz, and F. Steglich, Hall effect in the ferromagnet UGe₂, *Phys. Rev. B* **69**, 195314 (2004).
- [29] C.-Z. Li, J.-G. Li, L.-X. Wang, L. Zhang, J.-M. Zhang, D. Yu, and Z.-M. Liao, Two-carrier transport induced Hall anomaly and large tunable magnetoresistance in dirac semimetal Cd₃As₂ nanoplates, *ACS Nano* **10**, 6020 (2016).
- [30] K. Ueda, S. Hirose, and H. Asano, Ambipolar transport in Mn₂CoAl films by ionic liquid gating, *Appl. Phys. Lett.* **110**, 202405 (2017).
- [31] H. Yuan, H. Shimotani, J. Ye, S. Yoon, H. Aliah, A. Tsukazaki, M. Kawasaki, and Y. Iwasa, Electrostatic and electrochemical nature of liquid-gated electric-double-layer transistors based on oxide semiconductors, *J. Am. Chem. Soc.* **132**, 18402 (2010).
- [32] F. Hellman, A. Hoffmann, Y. Tserkovnyak, G. S. Beach, E. E. Fullerton, C. Leighton, A. H. MacDonald, D. C. Ralph, D. A. Arena, and H. A. Dürr, *et al.*, Interface-induced phenomena in magnetism, *Rev. Mod. Phys.* **89**, 025006 (2017).
- [33] See Supplemental Material at <http://link.aps.org/supplemental/10.1103/PhysRevApplied.17.034006> for details of reversibility, Hall effect of Pd, hole-carrier dominant Mn₂CoAl and gating effect on the Co₂MnCa.
- [34] E. C. Stoner, Collective electron ferromagnetism, *Proc. R. Soc. Lond. A. Math. Phys. Sci.* **165**, 372 (1938).
- [35] V. Stepanyuk, W. Hergert, K. Wildberger, R. Zeller, and P. Dederichs, Magnetism of 3d, 4d, and 5d transition-metal impurities on Pd (001) and Pt (001) surfaces, *Phys. Rev. B* **53**, 2121 (1996).
- [36] S. Shimizu, K. S. Takahashi, T. Hatano, M. Kawasaki, Y. Tokura, and Y. Iwasa, Electrically Tunable Anomalous

- Hall Effect in Pt Thin Films, *Phys. Rev. Lett.* **111**, 216803 (2013).
- [37] A. Obinata, Y. Hibino, D. Hayakawa, T. Koyama, K. Miwa, S. Ono, and D. Chiba, Electric-field control of magnetic moment in Pd, *Sci. Rep.* **5**, 14303 (2015).
- [38] L. Liang, Q. Chen, J. Lu, W. Talsma, J. Shan, G. R. Blake, T. T. Palstra, and J. Ye, Inducing ferromagnetism and kondo effect in platinum by paramagnetic ionic gating, *Sci. Adv.* **4**, eaar2030 (2018).
- [39] S. Skafiotouros, K. Özdogan, E. Şaşioğlu, and I. Galanakis, Generalized slater-pauling rule for the inverse heusler compounds, *Phys. Rev. B* **87**, 024420 (2013).
- [40] M. Weisheit, S. Fähler, A. Marty, Y. Souche, C. Poinsignon, and D. Givord, Electric field-induced modification of magnetism in thin-film ferromagnets, *Science* **315**, 349 (2007).
- [41] H. Nakayama, J. Ye, T. Ohtani, Y. Fujikawa, K. Ando, Y. Iwasa, and E. Saitoh, Electroresistance effect in gold thin film induced by ionic-liquid-gated electric double layer, *Appl. Phys. Express* **5**, 023002 (2012).
- [42] S. Dushenko, M. Hokazono, K. Nakamura, Y. Ando, T. Shinjo, and M. Shiraishi, Tunable inverse spin Hall effect in nanometer-thick platinum films by ionic gating, *Nat. Commun.* **9**, 3118 (2018).
- [43] T. Fujimoto, M. M. Matsushita, and K. Awaga, Electrochemical field-effect transistors of octathio[8]circulene robust thin films with ionic liquids, *Chem. Phys. Lett.* **483**, 81 (2009).
- [44] H. Yuan, H. Liu, H. Shimotani, H. Guo, M. Chen, Q. Xue, and Y. Iwasa, Liquid-gated ambipolar transport in ultrathin films of a topological insulator Bi_2Te_3 , *Nano Lett.* **11**, 2601 (2011).
- [45] T. McGuire and R. Potter, Anisotropic magnetoresistance in ferromagnetic 3d alloys, *IEEE Trans. Magn.* **11**, 1018 (1975).
- [46] J. Kudrnovský, V. Drchal, and I. Turek, Anomalous Hall effect in stoichiometric heusler alloys with native disorder: A first-principles study, *Phys. Rev. B* **88**, 014422 (2013).
- [47] H. Yuan, H. Shimotani, A. Tsukazaki, A. Ohtomo, M. Kawasaki, and Y. Iwasa, High-density carrier accumulation in ZnO field-effect transistors gated by electric double layers of ionic liquids, *Adv. Funct. Mater.* **19**, 1046 (2009).
- [48] T. Sugimoto, T. Katayama, Y. Suzuki, M. Hashimoto, Y. Nishihara, A. Itoh, and K. Kawanishi, Temperature dependence of perpendicular magnetic anisotropy in Co/Au and Co/Pt multilayers, *J. Magn. Magn. Mater.* **104**, 1845 (1992).
- [49] S. Song, C. Sellers, and J. Ketterson, Anomalous Hall effect in (110) Fe/(110) Cr multilayers, *Appl. Phys. Lett.* **59**, 479 (1991).
- [50] Z. Guo, W. Mi, R. Aboljadayel, B. Zhang, Q. Zhang, P. G. Barba, A. Manchon, and X. Zhang, Effects of surface and interface scattering on anomalous Hall effect in Co/Pd multilayers, *Phys. Rev. B* **86**, 104433 (2012).
- [51] C. Fang, C. Wan, Z. Yuan, L. Huang, X. Zhang, H. Wu, Q. Zhang, and X. Han, Scaling relation between anomalous nernst and Hall effect in $[\text{Pt}/\text{Co}]_n$ multilayers, *Phys. Rev. B* **93**, 054420 (2016).
- [52] A. Gerber, A. Milner, A. Finkler, M. Karpovski, L. Goldsmith, J. Tuailon-Combes, O. Boisron, P. Mélinon, and A. Perez, Correlation between the extraordinary Hall effect and resistivity, *Phys. Rev. B* **69**, 224403 (2004).
- [53] D. Zhang, H. Ishizuka, N. Lu, Y. Wang, N. Nagaosa, P. Yu, and Q.-K. Xue, Anomalous Hall effect and spin fluctuations in ionic liquid gated SrCoO_3 thin films, *Phys. Rev. B* **97**, 184433 (2018).
- [54] H. Ishizuka and N. Nagaosa, Spin chirality induced skew scattering and anomalous Hall effect in chiral magnets, *Sci. Adv.* **4**, eaap9962 (2018).
- [55] N. Nagaosa, J. Sinova, S. Onoda, A. H. MacDonald, and N. P. Ong, Anomalous Hall effect, *Rev. Mod. Phys.* **82**, 1539 (2010).
- [56] H. C. Koo, S. B. Kim, H. Kim, T.-E. Park, J. W. Choi, K.-W. Kim, G. Go, J. H. Oh, D.-K. Lee, and E.-S. Park, *et al.*, Rashba effect in functional spintronic devices, *Adv. Mater.* **32**, 2002117 (2020).
- [57] Y. Hibino, T. Koyama, A. Obinata, K. Miwa, S. Ono, and D. Chiba, Electric field modulation of magnetic anisotropy in perpendicularly magnetized Pt/Co structure with a Pd top layer, *Appl. Phys. Express* **8**, 113002 (2015).
- [58] S. Zhao, Z. Zhou, C. Li, B. Peng, Z. Hu, and M. Liu, Low-voltage control of $(\text{Co}/\text{Pt})_x$ perpendicular magnetic anisotropy heterostructure for flexible spintronics, *ACS Nano* **12**, 7167 (2018).
- [59] Y. Wang, F. Liu, C. Cao, C. Zhou, G. Chai, and C. Jiang, Ionic-liquid gating controls anomalous Hall resistivity of Co/Pt perpendicular magnetic anisotropy films, *J. Magn. Magn. Mater.* **491**, 165626 (2019).
- [60] Y. Zhang, Y. Yin, G. Dubuis, T. Butler, N. V. Medhekar, and S. Granville, Berry curvature origin of the thickness-dependent anomalous Hall effect in a ferromagnetic weyl semimetal, *npj Quantum Mater.* **6**, 17 (2021).
- [61] B. Ludbrook, B. Ruck, and S. Granville, Perpendicular magnetic anisotropy in Co_2MnGa and its anomalous Hall effect, *Appl. Phys. Lett.* **110**, 062408 (2017).